

2

In Vivo Applications of Quantum Dot Nanoparticles for Optical Diagnostics and Therapy

¹Elnaz Yaghini*, ²Alexander M. Seifalian, ¹Alexander J. MacRobert

¹Dr. E. Yaghini and Prof. A. J. MacRobert, Division of Surgery & Interventional Science and UCL Institute for Biomedical Engineering, University College London, London, UK.

²Prof. A. M. Seifalian Centre for Nanotechnology and Regenerative Medicine, Division of Surgery and Interventional Science, University College London, London, UK.

Outline:

Introduction.....	22
<i>Quantum Confinement and Size-tunable Properties of QDs</i>	22
<i>Bulk Semiconductor Physics</i>	23
<i>Synthesis and Bioconjugation of QDs</i>	24
<i>Photophysical Properties of qds and Comparison with Organic Dyes</i>	25
<i>IN VIVO STUDIES of QDs</i>	26
<i>Non-targeted In Vivo Imaging</i>	27
<i>Sentinel Lymph Node (SLN) Mapping</i>	27
<i>Passive Tumour Targeting</i>	29
<i>Targeted In Vivo Imaging</i>	30
<i>Active Tumour Targeting using Antibodies</i>	30
<i>Active Tumour Targeting using Peptides</i>	31
<i>In Vivo Imaging Using Self-illuminating qds (BRET)</i>	33
<i>Multifunctional QDs</i>	34
<i>Dual-modality Imaging</i>	34
<i>Integration of Imaging and Therapy</i>	34
<i>Cell Tracking</i>	35
<i>Future perspective</i>	36
<i>Improving the Biocompatibility of QDs</i>	36
<i>Potential Toxicity of QDs</i>	38
<i>Conclusions</i>	40
<i>References</i>	40

Introduction

Nanotechnology is a new field of interdisciplinary research on the fabrication of materials with nanoscale dimensions between 1-100 nanometre (nm) [1]. As the sizes of organic and inorganic materials are decreased toward the nanometre scale, their optical, electronic, magnetic and structural properties largely vary from that in the bulk and become size and shape dependent. Such size and shape dependent properties of nanomaterials make them attractive to a diverse range of applications ranging from energy conversion towards biomedical imaging and nanomedicine.

Semiconductor quantum dots (QDs) are tiny light-emitting particles on the nanometre scale, which are emerging as a new class of fluorescence probe for *in vivo* bimolecular and cellular imaging. These nanometre-sized crystalline particles are nanocrystals of inorganic semiconductors with a generally spherical shape. The core of the semiconductor material is synthesised with sizes in the range of 2-10 nm and contains hundreds of thousands of atoms of group II and VI elements (e.g. CdSe, CdTe) or group III and V elements (e.g. InP). The core is typically enclosed within a shell of another semiconductor that has a larger bandgap (Fig. 2.1).

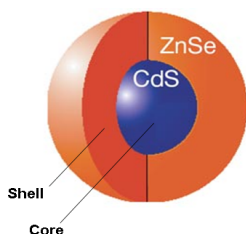


FIGURE 2.1

Schematic illustration showing the core/shell structure of quantum dots

QD nanoparticles are highly efficient fluorophores with a size-dependent emission wavelength, which due to quantum confinement increases with increasing size of the QD. Their extreme brightness and resistance to photobleaching enables the use of very low light intensities over extended time periods, making them especially useful for live-cell imaging [2]. Due to the unique photophysical properties of QDs, progress in synthesis and biofunctionalisation of QDs has generated an increasingly widespread interest in the fields of biology and medicine. Recently a wide range of methods for bio-conjugating colloidal QDs in a diverse area of applications have been developed such as cell labelling, cell tracking, *in vivo* imaging, DNA detection, and multiplexed beads [3-10]. This chapter is intended to provide an overview of the *in vivo* applications of QDs as well as the future direction for the development of optimised QD nanoparticles for their clinical translation.

Quantum Confinement and Size-tunable Properties of QDs

One of the most intriguing features of QDs is that by altering the QD size and its chemical composition, fluorescence emission can be tuned from the near ultraviolet, throughout the visible and into the near-infrared (NIR) spectrum, spanning a broad wavelength range of 400–2000 nm [11-13]. To understand these properties, the photophysics of bulk phase semiconductors will be discussed in following sections.

Bulk Semiconductor Physics

Based on electron conductivity, solid state physics typically divides materials into three well known categories: conductors (metals), semiconductors and insulators. The difference in the energy level between the valence and conduction band determines the conductivity of the solid materials. The valence band is the highest electronic energy level that is occupied with electrons at room temperature (Fig. 2.2). Likewise, the conduction band is the lowest energy electronic state that is not occupied by electrons. An electron in the valence band may gain energy (thermally or by the absorption of a photon) to enter the conduction band, thus vacating a positively charged hole in the valence band. The difference in energy between the valence and conduction bands, called the bandgap energy (e.g. typically expressed in electron volts [eV]), determines the energy that must be gained for an electron to enter the conduction band [14]

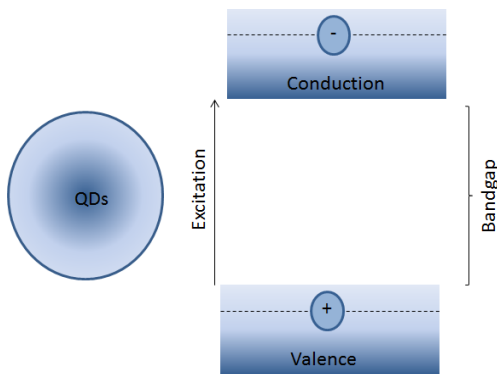
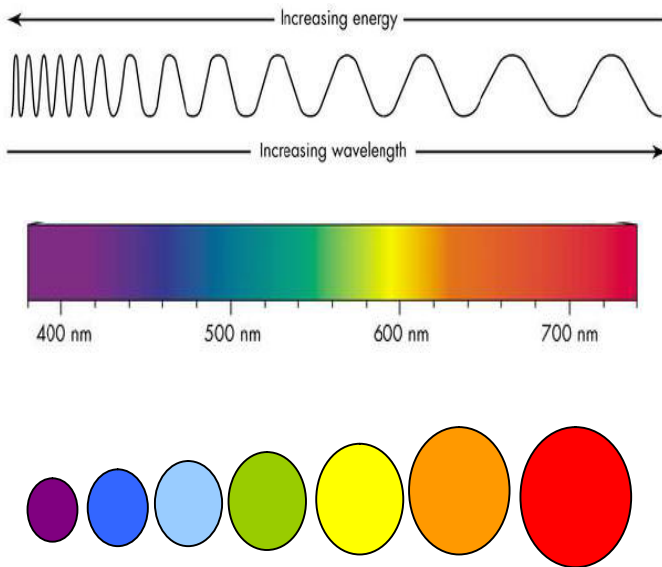


FIGURE 2.2

A schematic representation of the valence and conduction band of QD nanoparticles

The raised electron and the hole taken as a pair is called an “exciton”. Once in the excited state (electron in conduction band), a conduction-band electron may relax back to its ground state in the valence band through radiative recombination with a hole, resulting in the emission of a photon with the same energy as the bandgap. Light emission is only one of the many possible decay processes, but it is of both fundamental and practical importance.

QDs as semiconductor materials exhibit size-dependent energy state due to the confinement of the charge carriers (electrons-holes) in three dimensions. As the size of the QD decreases, the band gap increases, resulting in shorter wavelength of light emission (Fig. 2.3). Because the bandgap determines the fluorescence emission wavelength of semiconductor materials, considerable effort has been devoted to engineer fluorescence emitters with precisely tuned bandgaps. An intriguing property of semiconductors is that the bandgap is not only dependent on size but also on the particle composition [15]. Therefore, the composition of the material may also be used as a parameter to alter the bandgap of a semiconductor.

**FIGURE 2.3**

Size tunable optical properties of QDs illustrating the increase in emission wavelength with increasing quantum dot size

Synthesis and Bioconjugation of QDs

In the design of QDs, the selection of a core QD composition is determined by the desired wavelength of emission. Among various methods described in the literature, the highest quality QDs are typically prepared at elevated temperatures ($\sim 300^{\circ}\text{C}$) in organic solvents such as tri-*n*-octylphosphine oxide (TOPO) and hexadecylamine, both of which are high boiling point solvents containing long alkyl chains. These hydrophobic organic molecules perform as the reaction medium (solvent), and the basic functional groups (phosphine, phosphine oxides and amine) coordinate with unsaturated metal atoms on the QD surface to prevent the formation of bulk semiconductors. As a result, the nanoparticles are capped with a monolayer of the organic ligands and are soluble only in nonpolar hydrophobic solvents such as chloroform and hexane. A shell of another semiconductor such as ZnS or CdS with a wider bandgap is grown on the core surface to provide electronic insulation. The growth of a semiconductor shell on the surface of the core has been shown to significantly increase the fluorescence efficiency and quantum yield of QDs. It has also been shown that a ZnS shell is less susceptible to surface oxidation and therefore enhances the chemical stability of the QDs and decreases the oxidative photobleaching of QDs to a great extent [16;17].

For use in biological systems, QDs must be rendered hydrophilic so that they are soluble for aqueous formulations. Two general strategies have been developed to disperse QDs in aqueous solutions. In the first approach, the hydrophobic monolayers of the ligands on the QD surface are exchanged with hydrophilic ligands, such as mercaptoacetic acid [18;19]. However, this method has some drawbacks such as particle aggregation and precipitation in biological buffers and change in photophysical properties of QDs [18;20]. Alternatively, the native hydrophobic ligands (TOPO) can be retained on the QD surface, and rendered water soluble through the adsorption of amphiphilic polymers [4;21]. In this

method the coordinating organic ligands (TOPO) are preserved on the inner surface of the QD, a feature which is imperative for maintaining the optical properties of QDs and shielding the toxic elements of the core from the outside environment by a hydrocarbon bilayer. Although this method preserves the optical properties of QDs, the overall size of the particles after coating is rather large which could place a restriction on biological applications. Furthermore, the surface of water-soluble QDs can be functionalised with biomolecules such as antibodies, oligonucleotides or small molecule ligands for specific targeting. The surface of QDs may also be modified with hydrophilic molecules such as polyethylene glycol (PEG) to eliminate possible non-specific binding or to increase their circulation times in the bloodstream following intravenous injection.

Photophysical Properties of QDs and Comparison with Organic Dyes

Fluorescence techniques are very well suited to study many fundamental cellular processes where specific fluorescence probes are widely used in cell biology [22;23]. However, traditionally used fluorophores, in particular organic fluorophores, have their limitations. These molecules generally have narrow absorptions with asymmetric, broad emission spectra and low photobleaching thresholds [24]. Due to these intrinsic photophysical properties, traditional fluorescence probes have limited applications with regards to long-term imaging and multiplexing. QDs have several dramatically different properties compared to organic fluorophores, as was reviewed by Resch-Genger et al. [25]. Table 2.1 compares photophysical properties of QD nanoparticles versus organic dyes.

QDs have continuous broad absorption spectra that gradually increase in intensity towards shorter wavelengths, enabling excitation by a wide range of wavelengths (below the first exciton absorption band). Their emission spectra are symmetric and narrow, spanning the UV to near-infrared. Consequently, QDs of different sizes can be excited by a single wavelength, with minimal signal overlap. These differences provide QDs with several distinct advantages over organic fluorophores. Firstly, a narrow emission spectrum provides the possibility of distinguishing multiple fluorophores simultaneously. Secondly, the broad excitation spectrum of QDs facilitates the use of a single excitation wavelength (light source) to excite QDs of different colours. These unique features of QDs allow the simultaneous detection of different colour QDs, enabling several cells to be tracked *in vivo* [26;27], and the simultaneous bio-sensing of multiple molecules *in vitro* [28]. Furthermore, owing to the efficient multicolour excitation cross-section of QDs and the ability to synthesis QDs that can emit infrared or near-infrared light, QDs are highly suited for imaging cells deep within tissues [27;29]. The molar absorption coefficients at the first absorption band of QDs are generally larger compared to organic dyes [30]. The large molar extinction coefficient of QDs makes them brighter probes under photon-limited *in vivo* conditions where light intensities are severely attenuated by scattering and absorption. Following light exposure, organic fluorophores can also undergo light-induced reactions leading to irreversible change in their photophysical properties; a phenomenon known as “photobleaching”. This limits their application for long-term imaging. On the other hand, QDs are very stable light emitters owing to their inorganic nature, making them exceptionally resistance towards photo- and chemical degradation [4;26;31;32]. This excellent photostability makes QDs very effective probes not only for imaging QD-tagged proteins over long periods [33;34] but also for imaging the growth and development of organisms for periods ranging from weeks to months [26;29]. In addition, the two-photon cross-section of QDs is significantly higher than that of organic fluorophores making them quite well-suited for examination of thick specimens and *in vivo* imaging owing to deeper penetration of near-infrared excitation light [35;36]. Another important characteristic of QDs is their fluorescence lifetime of 10-100 nanoseconds (ns), which is significantly longer than typical organic dyes or auto-fluorescent proteins that decay in the order of a few nanoseconds [37;38]. The longer excited lifetime

of QDs provides a means to separate the QD fluorescence from short-lived background fluorescence using time-gating techniques. It also worth noting that bioconjugated QD probes are similar in size to fluorescence protein and do not suffer from major kinetic or steric hindrance problems [8;34].

TABLE 2.1

Photophysical properties of fluorescent organic dyes versus quantum dots

Property	Organic dyes	QDs
Absorption spectra	Narrow, discrete bands	Broad, steadily increasing toward UV wavelength
Molar absorption coefficient	$2.5 \times 10^4 - 2.5 \times 10^5 \text{ M}^{-1} \text{ cm}^{-1}$	$10^5 - 10^6 \text{ M}^{-1} \text{ cm}^{-1}$
Emission spectra	Asymmetric, with red tail	Symmetric
Quantum yield	0.5-1.0 (visible), 0.05-0.25 (NIR)	0.1-0.8 (visible), 0.2-0.7 (NIR)
Fluorescence lifetime	1-10 ns, mono-exponential decay	10-100 ns, typically multi-exponential decay
Two-photon cross section	$1 \times 10^{-52} - 5 \times 10^{-48} \text{ cm}^4 \text{ s photon}^{-1}$	$2 \times 10^{-47} - 10^{-46} \text{ cm}^4 \text{ s photon}^{-1}$
Size	~0.5 nm, molecule	2-10 nm, colloid
Photochemical stability	Low photobleaching threshold	High photobleaching threshold
Toxicity	From very low to high, dependent on dye	Limited known yet (potential nanotoxicity)
Spectral multiplexing	Not ideal due to the spectral overlap	Ideal for multi-colour experiments

IN VIVO STUDIES of QDs

QD nanoparticles are emerging as a new contrast agent in the biological system and have been receiving increasing attention for potential use in biology and medicine [10;39]. *In vivo* fluorescence imaging visualises the fluorescence emission from fluorophores in whole-body of living small animals. Although traditionally used near-infrared dyes such as Indocyanine green continue to be used, the development of fluorescent QD nanoparticles for *in vivo* fluorescence imaging offers several advantages [40]. The unique optical properties of QDs for *in vivo* imaging include: high absorption coefficient, high fluorescence quantum yield, and high resistance to photobleaching. More importantly, broad absorption and narrow emission spectra of QDs make them suitable for simultaneous multiplex imaging. Optical imaging presents itself as a powerful technique in image-guided therapy. However, optical imaging in live animals remains hampered by the limited penetration depth of visible light in the body. This limitation stems from the high absorption and autofluorescence that occur in biological tissue across most of the electromagnetic spectrum. In the near-infrared region (700-900 nm) the influence of the main tissue absorbing components, oxy and deoxyhaemoglobin ($\lambda_{\text{max}} < 600 \text{ nm}$) as well as water ($\lambda_{\text{max}} > 1150 \text{ nm}$) is minimal. As a result, contrast agents that emit in the near-infrared region (700-900 nm) of the spectrum can overcome this problem of penetrating deeper into the tissue and

out than UV, visible, or infrared light do [41;42]. Therefore optical imaging agents should ideally emit in the near-infrared region (700-900 nm) so that they can be used clinically. Few organic dyes are currently available that emit in the near-infrared region and they suffer from the same photobleaching problems as their visible counterparts. One of the greatest advantages of QDs for imaging in living tissue is their size/composition-dependent emission wavelength and their high two-photon absorption cross section and high photobleaching threshold. Consequently, development of far red/near-infrared QDs can overcome the limitation of organic fluorescence dyes. Several groups have thus synthesised biocompatible near-infrared emitting QDs as a fluorescence probe for *in vitro* and *in vivo* labelling [43]. In general, methods for designing fluorescence imaging probes can be divided into non-targeting and targeting. Due to their high surface area to volume ratio, QDs can be actively targeted to the desired tissues with antibodies, peptides or passively via the enhanced permeability and retention (EPR) effect. More importantly, QD nanoparticles offer multifunctionality, such as combining both imaging and drug delivery or dual modality imaging combining near-infrared and magnetic resonance imaging. The *in vivo* applications of QDs are summarised below with future opportunities and directions for their clinical translation.

Non-targeted In Vivo Imaging

Sentinel Lymph Node (SLN) Mapping

Cancer spreads in a variety of ways, by direct extension, via the vascular system and via the lymphatics/lymph nodes. The sentinel lymph node (SLN) is the first lymph node that drains from the primary tumour. There is generally orderly progression of cancer from the primary tumour to the SLN and then to the echelon lymph nodes. SLN localisation is one of the common methods used to identify the presence of cancer in a single lymph node and is particularly important for the treatment of melanoma, breast, cervical and head and neck cancers [44-46]. The techniques currently used for SLN mapping employ a radioactive tracer, or a blue dye for visualisation of lymphatic vessels. But these techniques are non-specific during surgery, which leads to unnecessary removal of lymph nodes, causing unwanted trauma such as lymphoedema and nerve damage. In addition some adverse reactions has been reported in patient following administration of the blue dye [47]. The potential radiation hazards and the overall procedure duration are other limiting factors for these techniques. The ideal method for SLN mapping should be accurate, rapid, and noninvasive. QD nanoparticles could be ideal probes for SLN mapping because they are highly fluorescent, non-radioactive and easily visible deep within tissues since QDs with strong red or near-infrared emission can be used where haemoglobin absorption is minimal. Intraoperative imaging permits removal of the SLNs during surgery. Using this technique it appears that near-infrared QD nanoparticles have the potential to revolutionise human cancer surgery by providing sensitive, specific, and real time intraoperative visualisation of normal and disease processes. Fig. 2.4 displays a schematic depiction of an intraoperative imaging set-up for real time fluorescence imaging of the surgical field. This enables surgeon with instantaneous imaging of lymphatic flow and provides real time visual feedback for image-guided localisation and dissection [48].

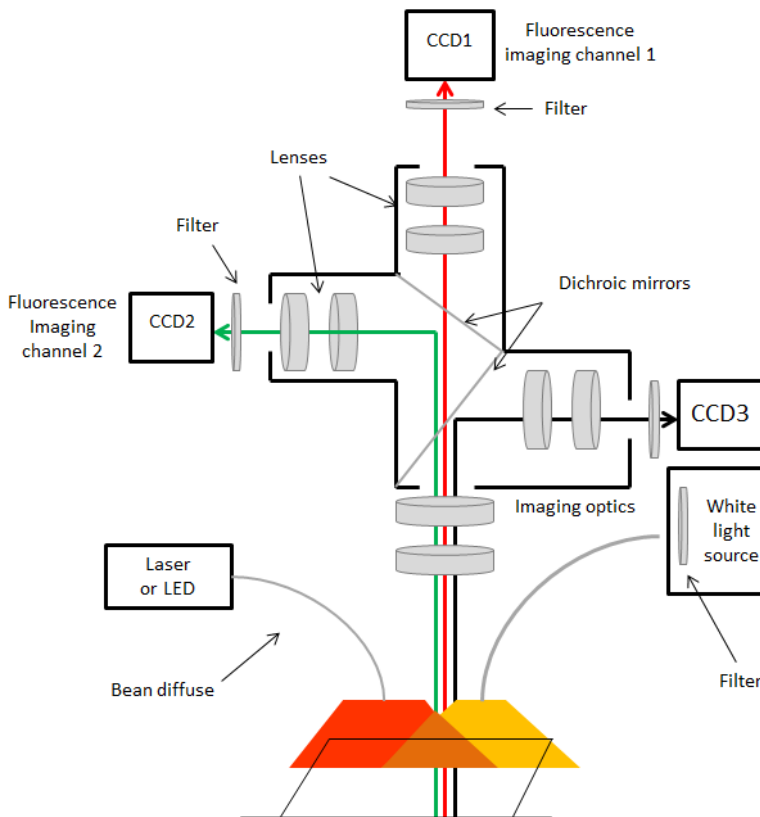


FIGURE 2.4

Multispectral intraoperative camera system. A laser or light-emitting diode is used to excite the fluorescence. The red QD fluorescence is imaged in one CCD camera channel, and tissue autofluorescence which occurs at shorter wavelengths with another camera. A colour image of the target field is also obtained using white light illumination and a third camera

For the lymphatic system the overall size of the nanoparticle is an important parameter in determining the biodistribution and clearance of QDs. Frangioni and colleagues used near-infrared emitting CdTe/CdSe core/shell QDs with a hydrodynamic size of 15-20 nm and demonstrated SLN mapping of QDs when injected intradermally into the paw of a mouse [29]. They also injected near-infrared QDs intradermally on the thighs of pigs and followed lymphatic flow towards the SLN in real time. Using excitation fluence rates of only 5 mW/cm^2 , within 5 minutes localisation of QDs in the SLNs was identified [29]. In subsequent studies, this group has demonstrated QD fluorescence imaging of lymph nodes draining the lungs [49;50], oesophagus [51] and gastrointestinal tract [52]. In another study, Zimmer et al. utilised very small PEG encapsulated near-infrared emitting QDs, with a hydrodynamic diameter of 10 nm [53]. When these QDs were injected into the paw of a mouse a sequence of draining lymph nodes was labelled instead of remaining trapped in SLNs. The authors concluded that migration through the first draining lymph node was due to the small size of their QDs. The multiplexing capabilities of QDs have also been exploited for mapping complex network of lymphatic vessels. Kobayashi et al. demonstrated utility of simultaneous multicolour fluorescence imaging of five different lymphatic basins using five types of near-infrared QDs with different emission spectra [54]. This is only possible with QDs due to their narrow and symmetric emission wavelength and broad absorption

spectra. Ballou et al. were amongst the first to inject the QDs into the tumours to map SLNs. In their study PEG encapsulated QDs with various charged groups were injected into the tumours of mice [55]. They demonstrated that tumour injection of QDs resulted in rapid migration of QDs from the tumour through lymphatics to surrounding lymph nodes which was visible through the skin. In their study, terminal charged groups had almost no effect on the extent of the drainage and pattern of the migration of QDs from the tumour to the adjacent lymph nodes. In study by Marchal et al. the detection of the SLN and the toxicity of the cadmium containing QDs (CdTeSe/CdZnS) were compared with cadmium free counterparts (CuInS₂/ZnS) [56]. In their work both types of QDs were injected subcutaneously in to the paw of healthy mice and were localised in the axillary lymph node in few minutes after the injection. Cadmium-based QDs clearly showed signs of toxicity such as increased lymph node weight with several inflammation sites. However, Cadmium-free QDs did not show any features of toxicity under the same conditions. In another study silicon QDs (Si QDs) with hydrodynamic of 20 nm were injected subcutaneously to the mice [57]. Following the injection QDs were observed in the axillary lymph nodes and no adverse effect was observed in mice from the injection of the Si QDs indicating their biocompatibility as a fluorescence probe for imaging.

In conclusion, the non-invasive fluorescence detection of SLN using QDs offers an opportunity to track lymphatic flow in real time and guide their nodal dissection after intraoperative injection. Using QDs it only takes a few minutes to detect the SLN. The QDs then slowly leaks from the injection point and the SLN into the rest of the body via lymphatic and blood circulation. This gives the surgeon a few hours to resect both the SLN and the injection point. Therefore at the same time the large majority of QDs are removed from the body which limits concerns regarding toxicity of QDs. Ideally the QDs should be targeted to the malignant tissue to maximise specificity, and there are several ways of achieving this as follows.

Passive Tumour Targeting

Under *in vivo* conditions QDs can be delivered to tumours by both passive and active targeting via the vasculature. In passive extravasation there is no need for special surface chemistry since nanometre-sized particles accumulate preferentially at tumour sites through the enhanced permeability and retention (EPR) effect [58]. This effect is believed to arise from two factors: (i) angiogenic tumours over express vascular endothelial growth factors that increase vascular permeability in tumours and cause leakage of circulating macromolecules and small particles; and (ii) lack of effective lymphatic drainage system, which leads to accumulation of macromolecules and nanoparticles [59;60]. Several studies have shown that QD nanoparticles can accumulate in the tumour due to the EPR effect [35;61]. For example, in a study by Gao et al. *in vivo* passive tumour targeting of QDs was reported and it was demonstrated that targeting was dependent on the stability of the QD in biological systems and its circulation time [35]. In their study PEG encapsulated QDs were taken up readily via passive delivery by tumours compared to carboxyl functionalised QDs. The observed findings were related to the increased circulation time and reduced non-specific adsorption of serum proteins due to the PEG encapsulation. The negatively charged nature of carboxylic acid terminated QDs enhanced their reticuloendothelial uptake and therefore hampered their tumour uptake. In a recent study by Shuhendler and colleagues [62], near-infrared emitting QDs encapsulated in solid fatty ester (QD-FEN) was used for *in vivo* imaging in a breast tumour-bearing animal model. *In vivo* animal imaging revealed that fatty ester encapsulated QDs surprisingly did not accumulate in the liver. They found that these QDs mainly accumulated in the spleen and their accumulation was observed to decrease to nearly preinjection levels by 96 h after injection. They stated that the encapsulation of QDs in fatty ester nanoparticles enhanced the biocompatibility of QDs by providing complete clearance of the QDs from the body. Furthermore, the

results showed that by 1 h after QD-FEN injection fluorescence signal of QDs in the tumour sites was detected, indicating the passive uptake of QD-FEN within the tumour tissue. The size and shape of the nanoparticles play an important role in this process and it has been shown that smaller particles penetrate deeper into the tumour interstitial medium [63]. Thus to obtain efficient tumour targeting without selective targeting several parameters should be considered in designing the QD nanoparticles. The design considerations should also focus on the development of highly stable and biocompatible QDs with long circulation times.

Targeted In Vivo Imaging

Active targeting can be efficient and is not necessarily affected by the degree of tumour vascular leakiness which differs according to the tumour locations. In active targeting, the QD surface is decorated with a ligand that selectively binds to surface receptor sites in the extracellular environment that play key roles in tumour proliferation, angiogenesis and metastasis. Many of these recognition sites exist in normal tissue but are significantly upregulated in numerous tumour cells of certain cancer types and offer a means of preferentially targeting the circulating QDs to tumours. The choice of ligand for active targeting plays a crucial role in the performance of the QD nanoparticles. The degree of selectivity, the strength of the interaction, the overall probe size, QD charge density and targeting ligand accessibility are all important factors that should be considered. For instance in a study by Bawendi et al. it has been shown that a maximum hydrodynamic diameter of about 5.5 nm is required for renal excretion of QDs within 4 h [64]. They also reported that QDs with high charge-to-hydrodynamic diameter ratios can cause adsorption of serum proteins and increase the hydrodynamic diameter [64]. Bawendi et al. have suggested that a zwitterionic coating can reduce nonspecific adsorption on the QD surface because of the low net charge density [65]. It should also be noted that the penetration of QDs from vasculature into tumour can be affected by the overall size of the QDs. Large targeting ligands such as antibodies (Abs) may lead to probe accumulation in tumour vasculature with little or no tissue penetration, despite the high selectivity and affinity of the antibodies as targeting agents. Therefore, careful consideration must be given to the design of specific targeting ligands. The following section describes examples of active targeting of tumour *in vivo* using peptides and proteins.

Active Tumour Targeting using Antibodies

Active targeting can be obtained by binding to receptor sites recognised by antibodies and other proteins such as epidermal growth factor (EGF). The main disadvantages of employing proteins as targeting agents arise from the size of the proteins as ligands and the resulting size of the QD conjugates. Some examples of protein-mediated active targeting of QDs are given below.

In a study by Gao et al. PEG encapsulated QDs were bioconjugated with a specific antibody (antibody against the prostate-specific membrane antigen: PSMA) and were injected into the tail vein of mice bearing subcutaneous human prostate cancer [35]. They demonstrated that tumour targeting was much faster and more efficient for the targeted QDs compare to un-targeted QDs, which accumulated in tumour sites passively via the EPR effect. In a similar approach by Yu et al. QD nanoparticles were conjugated with a specific antibody against an important marker for hepatocellular carcinoma [66]. Upon intravenous injection of QDs into the mice bearing hepatocellular carcinoma, active tumour targeting of bioconjugated QDs was observed in tumour sites where their uptake was considerably higher than that of un-targeted QDs due to passive targeting.

Tada et al. used QDs to study the biological process involved in active targeting of nanoparticles to the tumour [67]. In their study, QD nanoparticles were labelled with antibody against human epidermal growth factor receptor 2 (HER2) and administered intravenously into mice with HER2-overexpressing breast cancer implanted tumours. Upon systemic delivery of QDs their migration from injection sites to the tumour sites was monitored, using intravital fluorescence microscopy. The QDs circulated in the bloodstream, extravasated into the tumour, diffused in extracellular matrix, bound to their receptors on tumour cells, moved from the cell membrane to the perinuclear region, and then localised in the perinuclear region of the cells. Therefore, the combination of sensitive QD probes with methods such as real time microscopy for *in vivo* animal imaging could provide new insights into the understanding of tumour biology and processes involved in the transport of drug carriers.

Active targeting of QDs to tumours has also been reported by the use of epidermal growth factor receptor (EGFR). EGFR is a transmembrane protein that plays an important role in tumour progression and proliferation. EGFR becomes highly upregulated in many cancer types which provides an opportunity for designing a receptor targeted approach for the detection and treatment of cancer [68;69]. In a study by Yang et al. single-chain epidermal growth factor receptor antibody (ScFvEGFRA) was conjugated with QDs and paramagnetic iron oxide (FeO) nanoparticles to image human pancreatic cancer in mice [70]. Targeted and untargeted QDs were injected intravenously into mice and their biodistribution was studied using fluorescence microscopy. Strong QD fluorescence signal was detected in the cytoplasm of tumour cells from the mice that received ScFvEGFRA-QD but not untargeted QDs. Strong fluorescence signals were obtained from normal tissues of the mice that were injected with untargeted QDs, whereas the QD fluorescence from normal tissues of the mice that received targeted QDs was negligible. These findings indicated the potential of ScFvEGFRA conjugated nanoparticles for the detection of EGFR-expressing tumours using *in vivo* imaging approach.

Overall, these results imply that targeted nanoparticles have the potential to be used as effective agents for *in vivo* tumour imaging. Efficient intracellular delivery of targeted nanoparticles can also be used for specific delivery of therapeutic agents.

Active Tumour Targeting using Peptides

The small size of peptides relative to antibodies makes them attractive as targeting ligands. One of the earliest examples of active targeting of QDs using peptide conjugates was reported by Akerman et al. [71]. They demonstrated, for the first time, selective targeting of peptide coated QDs to the vasculature of normal lung and tumours *in vivo*. In their work three different thiolated peptides were conjugated with mercaptopropionic acid (MPA) coated QDs and injected intravenously into mice to target the lung blood vessels, tumour blood vessels and tumour lymphatic vessels. Using fluorescence microscopy, they showed that QDs coated with a lung-targeting peptide accumulated in the lungs of mice after intravenous injection, whereas two other peptides specifically directed QDs to blood vessels or lymphatic vessels in tumours.

Arginine-glycine-aspartate acid (RGD) peptide is one of the most widely used sequences for targeting tumours due to its high affinity for integrin [72]. The protein integrin, which binds to RGD containing components of the interstitial matrix, plays a key role in the progression of angiogenesis and metastasis. It is highly overexpressed on the surface of angiogenic endothelial cells and tumour cells of certain cancer types, making it attractive for tumour targeting [73;74]. *In vivo* targeting and imaging of tumour vasculature using arginine-glycine-aspartic acid (RGD) peptide-labeled QDs was investigated for the first time by Cai et al. [75]. In their work amine-modified QDs with peak emission at 705 nm (QD705) was conjugated to the thiolated RGD peptide resulting in the formation of QD705-RGD. Athymic nude mice bearing subcutaneous U87MG human glioblastoma tumours were administered

with QD705 and QD705-RGD intravenously. *In vivo* fluorescence imaging of U87MG tumour bearing mice showed that when mice were injected with QD705-RGD the fluorescence signal was detectable in the tumour as early as 20 min postinjection, which reached its maximum at 6 h postinjection. However, no significant fluorescence signal was observed in the tumour for the QD705 injected mouse. Successful tumour imaging indicated the specific *in vivo* targeting of integrin $\alpha_v\beta_3$ using QD705-RGD. *Ex vivo* fluorescence imaging also confirmed the uptake of QD705-RGD into the tumour. Microscopic images of frozen tumour slices stained for CD31 immunofluorescence staining showed that QDs were localised inside the vessels and did not extravasate, which was attributed to the large hydrodynamic diameter of these QDs.

In another study by Gao et al. [76] the specific tumour targeting of RGD peptide labelled near-infrared non-cadmium QDs was investigated. PEG encapsulated core/shell/shell QDs (QD800-PEG) with a peak emission wavelength at 800 nm were conjugated with RGD peptide (QD800-RGD). In their study QD800-PEG were also conjugated with the thiolated RAD peptide c(RADy(ϵ -acetylthiol)K) to produce QD800-RAD which was used as the negative control. Dynamic light scattering (DLS) analysis showed that the hydrodynamic diameter of QD800-PEG, QD800-RGD, and QD800-RAD were about 16.5 nm, 19.6 nm, and 20.1 nm, respectively. Animal experiments were performed on nude mice bearing subcutaneous U87MG human glioblastoma tumours. After intravenous injection of QD800-RGD, QD800-PEG, and QD800-RAD, the fluorescence signal of QDs was monitored at various time intervals using the IVIS Imaging System. Their results showed that after about 1 h postinjection of QD800-RGD, the fluorescence signal of the tumour reached maximum and then slightly decreased over time, while there was little to no tumour contrast in the mice injected with QD800-PEG or QD800-RAD. These results indicated highly specific tumour targeting of QD800-RGD. A bright fluorescence signal of QDs was observed in the liver, spleen and bone marrow, demonstrating the accumulation of QDs in the reticuloendothelial system sites which was due to the relatively short half-lives of these QDs. For *ex vivo* imaging, tumour and major organs were harvested and immediately were subjected to fluorescence imaging using the same imaging system. The *ex vivo* results further confirmed the obvious fluorescence signal in the U87MG tumour of mice injected with QD800-RGD, whereas there was almost no fluorescence signal in the tumours of mice administered with QD800-PEG or QD800-RDA. In their work although the uptake of the QDs in the liver was highest among all of the organs, the difference between tumour fluorescence signals indicated that only QD800-RGD has the capability to specifically target and detect U87MG tumour. Through CD31 immunofluorescence staining, performed to investigate the microscopic localisation of the QD in the tumours, fluorescence overlay images, showed the presence of QD800-RGD in the tumour vessels but no QD fluorescence signal in the tumour vessels of mice injected with QD800-PEG or QD800-RAD. Furthermore the images showed that QDs were localised inside the tumour and did not extravasate from the tumour vessels suggesting that QDs of greater size can only target the vascular integrin but not tumour cell integrin [71;75;77]. However, QDs with smaller sizes (<10 nm in hydrodynamic diameter) can facilitate their extravasation (due to the EPR effect), enhance the specific targeting to tumour cells and minimise the reticuloendothelial uptake [64;65;78;79].

Recently in a study by Gao J et al. [80] dendron-coated non cadmium containing core/shell QDs (QD710-Dendron) with peak emission at 710 nm were conjugated with RGD peptide (QD710-Dendron-RGD₂). Active tumour uptake of these QDs was investigated in nude mice bearing subcutaneous SKOV3 tumours. *In vivo* and *ex vivo* fluorescence imaging showed that the QD710-Dendron-RGD₂ nanoparticles resulted in high tumour uptake and long retention of these nanoparticles at tumour sites. The QD710-Dendron also displayed tumour accumulation, although to a lesser degree, which was likely caused by passive uptake of nanoparticles due to the EPR effect. In comparison to the QD710-Dendron-RGD₂, the fluorescence signal of QD710-Dendron at tumour sites was relatively low and decreased

significantly over time, and there was almost no tumour contrast after 24 h. The rapid change of tumour fluorescence signal in the mice injected with QD710-Dendron was attributed to a weak interaction of passive targeting. In their study anti-CD31 immunostaining of tumours was used to study the microscopic location of QDs in the tumour and the results revealed the presence of QD710-Dendron-RGD₂ both inside and outside tumour vessels. These findings indicate that QD710-Dendron-RGD₂ not only specifically binds to vascular integrin $\alpha_v\beta_3$ but also extravasates and interacts with integrin $\alpha_v\beta_3$ expressed on tumour cells. The extravasation of QD710-Dendron-RGD₂ was in contrast to previous work whereby using QDs with a hydrodynamic diameter larger than 20 nm they found no extravasation was observed [75-77;81]. They attributed this to the extravasation of QD710-Dendron-RGD₂ owing to their relatively small hydrodynamic diameter *in vivo*.

In Vivo Imaging Using Self-illuminating QDs (BRET)

The application of QDs in living systems can be limited due to the requirement of an external illumination source for excitation which produces strong background autofluorescence from endogenous chromophores. In addition, because of absorption and scattering of optical photons in tissues, little light could be available for QDs excitation at deep tissues. Moreover, there can be nonselective tissue damage at the illumination site at high laser powers. Therefore, an ideal QD would emit light without the need for the external excitation source. Towards these goals new types of QDs referred to as “*self-illuminating*” QDs have been explored. These QDs can fluoresce without the need for an external light source, based on the bioluminescence resonance energy transfer (BRET) process [82-84]. BRET is a naturally occurring process whereby a bioluminescent compound (the donor) nonradiatively transfers energy to a fluorescent compound (the acceptor) in close proximity [85;86]. BRET is analogous to Förster resonance energy transfer (FRET), except that the donor emission comes from a chemical reaction catalysed by an enzyme rather than from absorption of light from an external source, such as a laser. Efficient BRET occurs when there is an appropriate spectral overlap between the emission spectrum of the donor and excitation spectrum of the acceptor. BRET efficiency is inversely dependent on the sixth power of the distance between the donor and the acceptor, and therefore a short-range effect is typically a few nanometres. The unique photophysical properties of QDs such as broad absorption spectra, large molar extinction coefficient, high quantum yield and tunable emission spectra make them ideal acceptors for the BRET studies.

Near-infrared self-illuminating QD conjugates can emit light from red to near-infrared region in living cells and in living animals for deep tissue *in vivo* imaging. For instance, new types of self-illuminating QD conjugates have been developed by So et al. [82]. In their study carboxyl functionalised QDs were employed as the acceptor and coupled to a mutant of the bioluminescent protein *Renilla reniformis* luciferas (Luc8). They showed that the conjugates emit bioluminescent light in cells and in animals even in deep tissues. Upon the addition of the substrate coelenterazine or the protein emits blue light with a peak emission at 480 nm. The QD which was in close proximity with protein was excited nonradiatively via the BRET mechanism. They demonstrated coupling of the QD with the luciferase protein, and the emission from QDs was detected at subcutaneous and intramuscular sites in a mouse model. In addition, multiplex imaging was demonstrated by labelling three groups of cells with three different QD BRET conjugates injected into the same mouse. In another study, C6 glioma cells were labelled by QD-BRET conjugates and injected through the tail vein into the mouse [84]. Using BRET emission from QDs their trafficking into the lungs was imaged. In their study, multiplex imaging by labelling two groups of cells with two different QD BRET conjugates injected into the same mouse was demonstrated.

In general, by eliminating the need for the external light source for the excitation BRET offers a variety of advantages, including insignificant photobleaching of the fluorophores, no autofluorescence background and no direct excitation of the acceptor. With the ability to tune the emission of QDs simply by changing their size and composition, a variety of BRET pairs could be developed, which would make it possible for various interactions to be imaged concurrently in the same animals.

Multifunctional QDs

The large surface of QDs makes these nanoparticles suitable scaffolds to accommodate multiple imaging and therapeutic agents through chemical linkage or physical immobilization. This may enable development of multifunctional nanostructures for multimodality imaging and integrated imaging and therapy.

Dual-modality Imaging

Optical imaging is highly sensitive, though its application in humans and *in vivo* experimental models is hampered by limited tissue penetration depth, and poor anatomical resolution and spatial information. It is also difficult to sufficiently quantify QD signals in living subjects based on fluorescence intensity alone. To address these limitations, several groups have developed dual modality nanostructure by combining QD-based imaging with other imaging techniques such as positron emission tomography (PET) and magnetic resonance imaging (MRI) as described in the literature [87]. The most commonly used method to build multifunctional QDs are coating QDs or conjugating them with paramagnetic (for MRI) or radioactive (for PET) ion chelates or molecules. For example, Chen et al. developed a dual function imaging probe for both optical imaging and PET [77]. PET-detectable radionuclide ^{64}Cu was attached covalently to the polymeric coating of QDs. Targeted *in vivo* imaging of a subcutaneous mouse tumour model was obtained by additionally attaching arginine-glycine-aspartate acid (RGD) peptides on the QD surface. The ultrahigh sensitivity of PET imaging enabled the quantitative analysis of the biodistribution and targeting efficacy of this dual-modality imaging probe. This approach can overcome the tissue penetration depth limitation for QD imaging, therefore allowing quantitative *in vivo* targeted imaging in deep tissue and may facilitate future biomedical applications of QDs.

Another method to form multifunctional probes is doping the QDs with transition metals, such as Mn. For example in a study by Wang et al. water soluble core/shell CdSe/Zn_{1-x}Mn_xS nanoparticles were synthesised and were applied to the cells [88]. Using both MRI and fluorescence microscopy they demonstrated that QDs produced sufficient contrast in cells, indicating the utility of these nanoparticles for imaging. In a third approach fluorescence/paramagnetic nanoparticles were made by assembling QDs with Fe₃O₄ or FePt magnetic nanoparticles in silica beads, micelles, and polymer particles or within nanoheterostructures [89-91].

Integration of Imaging and Therapy

Drug-containing nanoparticles have shown great promise for treating tumours in animal models and in clinical trials [92]. QDs have also been utilised to carry distinct classes of therapeutic agents for simultaneous imaging and therapeutic applications. Farokhzad et al. developed a ternary system as a targeted cancer imaging, therapy, and sensing system [93]. In their study the QD surface was functionalised with an A10RNA aptamer (which recognises the extracellular domain of the prostate specific membrane antigen (PSMA)) to develop a targeted QD imaging system (QD-Apt). A well-known anti-cancer drug, Doxorubicin (Dox), was attached to the stem region of the aptamers, taking

advantage of nucleic acid binding ability of Doxorubicin. In this configuration, two donor-acceptor pairs of fluorescence resonance energy transfer (FRET) between QD-Dox and Dox-RNA aptamers occurred. They showed that this multifunctional nanostructure can deliver Doxorubicin to the targeted cells and monitor the delivery of Doxorubicin by activating the QD fluorescence, which simultaneously images the cancer cells.

The potential of QDs for photo-induced formation of reactive oxygen species (ROS) has been reported by several groups which is the basis of photodynamic therapy (PDT). Photodynamic therapy is a minimally invasive therapeutic modality approved for the clinical treatment of several types of cancer and non-oncological disorders. Generally, the photodynamic therapy procedure consists of administering the photosensitiser systemically (intravenous injection) or topically to the skin. Then, the diseased tissue is illuminated with light at an appropriate wavelength and energy dose at an appropriate time (when the photosensitiser concentration corresponds to a maximum accumulation in target tissue). The photosensitiser is activated by the light and interacts with molecular oxygen (O_2) to produce cytotoxic reactive oxygen species [94;95]. Most of the clinically and experimentally available photosensitisers have some major drawbacks such as instability in aqueous solutions, prolonged cutaneous sensitivity, chemical impurity, poor selectivity (in terms of targeting diseased tissue), low extinction coefficients, low photobleaching thresholds and weak absorption at the therapeutic wavelength [96]. To address these problems new photosensitisers are being sought together with improved delivery systems, including nanoparticle carrier systems. There has been an increasing number of reports on the preparation and utilisation of nanocarriers for photodynamic therapy agents [97-103]. Among the different nanoparticles that offer great promise in photodynamic therapy applications are QD nanoparticles. In relation to photodynamic therapy, QD nanoparticles possess several characteristics which make them attractive as a new therapeutic agent. For instance, their surface can be functionalised for specific targeting, they have large extinction coefficients, large two-photon cross sections and are exceptionally resistant to photobleaching [104].

Although targeted delivery of QDs in cancer cells and tumour tissue by using anticancer antibodies and other biomolecules has become possible recently, the efficiency of QDs on their own to produce ROS under direct photoactivation appears to be relatively low, compared with conventional photosensitiser drugs. Thus, in order to utilise the exceptional photostability, broad absorption band and large two-photon cross section of QDs beside improving the production of ROS, several groups have investigated the utility of quantum dot-photosensitiser complexes or hybrids as new generation drugs for photodynamic therapy [105-108]. In this configuration, the QDs act as energy donors and excite photosensitiser acceptors indirectly via the Förster resonance energy transfer (FRET). Based on the growing number of *in vivo* studies of QDs in experimental tumour models, there is clearly considerable potential for quantum dot-photosensitiser complexes in photodynamic therapy.

Cell Tracking

Cell tracking using QD nanoparticles is also a very active and promising area of research. The ability to track and target local tumour growth, distant metastasis, tumour associated neovasculature, and stem or immune cells in live subjects are crucial to many biological studies. For these purpose QDs should be able to efficiently label target cells *in vitro* and they should not leave the cells after *in vivo* injection. Several studies have shown that QDs remain inside their initial cells during the experiments. Dubertret et al. demonstrated for the first time the *in vivo* cell tracking using QD nanoparticles. In their study QDs were injected into the cytoplasm of single frog embryos. They showed that as the embryos grew, the cells divided, and each cell that descended from the original labeled cells retained a portion of the fluorescent cytoplasm, which could be fluorescently detected under illumination [4]. In another study

by Lei et al. PEG encapsulated CdSe/ZnS were conjugated with the HIV derived cell penetrating Tat-peptide and were introduced into living mesenchymal stem cells (MSCs) [109]. Using the confocal microscopy the results show that Tat-QDs could enter the MSCs efficiently. They also injected Tat-QDs intravenously into the mice and tissue distribution of these labelled stem cells was assessed with fluorescence microscopy. The results showed that Tat-QDs were observed in the liver, spleen and lung with little or no QDs in other organs. They demonstrated that labelled stem cells can be visualised at the single cell level, offering a promising application in stem cell transplantation and stem cell based therapy. Also Gao et al. loaded cancer cells with QDs and injected these cells subcutaneously into the mice [35]. They observed that implantation of QD-loaded cells led to normal tumour growth in animal model and the fluorescence of the QDs was detected through the skin. In another study human mesenchymal stem cells were loaded with QDs [110]. They showed that these cells could be implanted into an extracellular matrix patch for use as a regenerative implant for canine heart with a surgically induced defect. Eight weeks after implantation QD fluorescence were detectable in histological sections, indicating that the locations of these cells could be determine for at least eight weeks following delivery *in vivo*.

The ability to separate fluorescence from different type of QDs using multiphoton and emission-scanning microscopy provides the opportunity to study the interaction of different population of tumour cells and tissue cells within the same animal. For instance, in a study by Voura et al. tumour cells were labelled with QDs and were intravenously injected into mice [111]. In this study QDs and spectral imaging allowed the simultaneous identification of five different populations of cells using multiphoton laser excitation.

Future perspective

Improving the Biocompatibility of QDs

For most *in vivo* imaging studies using QD nanoparticles, systemic intravenous delivery of QDs is the main route of administration. For this reason, the interaction of nanoparticles with the plasma components, adsorption to blood cells and the vascular endothelium and the eventual biodistribution in various tissues are important factors. These parameters are particularly important when considering tumour-specific imaging applications.

Upon entering the body nanoparticles like other foreign pathogens, encounter multiple lines of defence that protect the body from invading substances. Adsorption of plasma proteins on the nanoparticle surface is called opsonisation [112]. This helps immune cells such as macrophages to recognise and take up the nanoparticles. Opsonisation could lead to a dramatic change in physicochemical properties of nanoparticles such as increased hydrodynamic size, aggregation and charge neutralisation. The phagocytic monocytes and macrophages, found around the body and largely in the liver, spleen, lymph nodes and bone marrow, collectively make up the reticuloendothelial system (RES). As a result of nanoparticle phagocytosis by macrophages in the blood and via these reticuloendothelial system organs, nanoparticles are commonly sequestered to these organs. The immune recognition of nanoparticles and their uptake by the reticuloendothelial system reduces their circulation time in the blood and can dramatically affect their drug delivery efficacy. This problem is particularly important for targeted nanoparticles that need time to bind to the tumour receptors and for non-targeted nanoparticles that rely only on the EPR effect.

There are several factors which influence *in vivo* QD biodistribution including the nanoparticle size, hydrophobicity, surface charge, the route of administration, and the physiological environment to

which nanoparticles are introduced. Most of the *in vivo* biodistribution studies of QD nanoparticles have demonstrated the accumulation of QDs in the RES such as liver, spleen. It has been shown that time-dependent accumulation of QDs in the RES was strongly dependent on the QD size, where the uptake was higher for larger particles. Furthermore, it has been revealed that the adsorption of serum proteins on the QD surface is dependent on surface coating, which can significantly increase the hydrodynamic diameter of QDs and subsequently their RES uptake. For instance, in a study by Bawendi et al. the hydrodynamic diameter of purely cationic or purely anionic QDs was enhanced by approximately 15 nm in the presence of serum [64]. In a subsequent study by this group it was demonstrated that neutral and hydrophilic polymer encapsulated QDs tended to avoid the serum protein adsorption, while maintaining permeability and retention in tumour sites [113]. In another study by Fischer et al. hydrophilic ligand exchanged QD, using mercaptopropionic acid exhibited hydrodynamic diameter growth from 25 nm to 80 nm in the presence of bovine serum albumin (BSA). However, zwitterionic cysteine encapsulated QDs did not change in size when subjected to fetal bovine serum [114].

Hence for successful targeted drug delivery and imaging, it is necessary to minimise opsonisation and prolong the circulation of nanoparticles *in vivo*. This can be achieved by surface coating of the nanoparticles with hydrophilic polymer/surfactants such as polyethylene glycol (PEG). Studies show that PEG confrontation at the nanoparticles surface is of utmost importance for the opsonin repelling function of the PEG layer. In the case of QD nanoparticles, numerous studies have also shown that PEG increases the colloidal stability of QDs in blood [64;113;115]. For instance, in a study by Gao et al. QDs were encapsulated with triblock copolymer and were linked to PEG [35]. *In vivo* targeting studies of human prostate cancer growing in nude mice showed an increase in the blood circulation time of these QDs which was proportional to the length of the PEG chain. In another study, near-infrared emitting QDs were ligand exchanged with dihydrolipoic acid (DHLLA) and conjugated with PEG chains with various lengths. Intermittent sampling from the tail vein revealed that low-molecular-weight PEGylated QDs had shorter blood circulation times compared to the larger molecular weight PEGylated QDs [113]. The same trend was reported by Al-Jamal et al. who found that blood retention times for larger molecular weight PEGylated QDs (PEG 2000-5000) was significantly longer than low-molecular-weight PEGylated QDs (PEG 750) [116].

It should be noted that the presence of a PEG coating may only delay the RES uptake of QD nanoparticles, since all nanoparticles are prone to eventually accumulate in the RES, irrespective of surface coating. The liver is considered the main organ for capturing nanoparticles greater than 10-20 nm [64]. It appears that liver uptake is dependent on the size of the nanoparticles: uptake of larger particles is greater and they are excreted from the body more slowly. For instance, 4 h after intravenous injection, the QD515 of hydrodynamic diameter of 4.4 nm were mainly found in the bladder, with less than 5% located in the liver. In contrast, 25% of the injected dose of the larger QD574 with hydrodynamic diameter of 8.7 nm was observed in the liver [64]. Similar results were reported by Fischer et al. where 90 min postinjection 99.5% of the injected dose of QDs coated with bovine serum albumin (hydrodynamic diameter: 80 nm) was found in the liver, whereas only 36% of the injected dose of QD coated with mercaptopropionic acid (hydrodynamic diameter: 25 nm) was found in the liver [114]. In another study that examined the effect of size, non-cadmium containing QDs were coated with two different carboxylate coatings, one with a hydrodynamic diameter of 25 nm (QD800-COOH) and the other with a hydrodynamic diameter of less than 10 nm (QD800-MPA). QDs were injected intravenously into mice bearing 22B and LS174T tumours. It was found that tumour uptake with QD800-MPA was higher than QD800-COOH, likely due to their smaller size. In addition it was revealed that smaller QDs were excreted from the body more efficiently than larger QDs. Fluorescence signals of QD800-MPA were detected in the kidney and bladder which decreased with time, indicating renal

clearance. In contrast, for the larger particles fluorescence signals were mainly found in the liver, bone marrow and spleen but tumour contrast was very low. The non-specific uptake of QD800-COOH particles was related to their larger size [79].

Surface coating determines the overall QD size, therefore high molecular weight polymers or organic coating lead to considerable increases in the QD diameter that can accelerate QD blood clearance and liver entrapment. From the clinical point of view, it would be possible to inhibit the accumulation of QDs and avoid potential toxic effects if they are within the size range that enables renal excretion. Studies have shown that the biodistribution and elimination of QDs are strongly correlated with QD size [64;65;113]. For example Frangioni et al. demonstrated that the renal clearance of QDs is closely related to their hydrodynamic diameter and the renal filtration threshold (~ 5.5 nm) [64]. Of equal importance to the QD size, is that the surface does not promote protein adsorption, which could significantly increase the QD diameter above that of renal threshold, and promote phagocytosis. They reported that the surface charge of QDs had an important effect on the overall size of QDs under physiological conditions. Purely positive or negative QD surface charge was related with an overall increase in the QD hydrodynamic diameter above 15 nm, due to the interaction with serum proteins. This increase prevented their renal excretion and led to the enhancement in their accumulation in liver. In their study only coated QDs with a hydrodynamic diameter of less than 5.5 nm were rapidly excreted in the urine and eliminated from the body.

In general, the metabolism and the excretion route of QDs still remain unclear and have to be investigated extensively. Ideally the small amount of the QDs remaining in the body should be ultimately eliminated, either via the kidneys into the urine or via the hepatobiliary pathway. The mechanisms for complete clearance are however not well understood yet.

Potential Toxicity of QDs

The major concern to the clinical translation of QDs is their toxicity due to their chemical composition of toxic heavy metal atoms (e.g Cd, Hg, Pb, As). Currently the most commonly used QDs contain cadmium. Although this element is incorporated into the core of the nanocrystal, surrounded by inert zinc sulphide, and encapsulated within a stable polymer, it is still unclear if this toxic ions can be used as clinical contrast agents. Therefore, despite potential biomedical applications of QDs concerns persists about their safety.

In vitro studies have shown that QD toxicity arises from several factors such as chemical composition, size, shape, surface charge, surface coating, and dose. Their ability for photo-induced formation of reactive oxygen species (ROS) and nanoparticle aggregation are other parameters involved in QDs toxicity [117-122]. Toxicology data derived from *in vitro* studies may not reflect the response of a physiological system to an agent. Animal model is the preferred system for the toxicological assessment of a novel agent. Therefore comprehensive *in vivo* toxicity evaluation of QDs is crucial for their clinical translation. *In vivo* toxicity is determined by several factors including dose, route of administration, metabolism, excretion rate, and immune response. Chemical composition, size, shape, aggregation and surface coating are also involved in QD-induced toxicity. Various animal models have been used to study *in vivo* toxicity of QDs and a few examples are described in the following sections [123].

Generally, mammalian models are used for the *in vivo* toxicity study, but recently some groups have used zebrafish for toxicity study of QDs. King-Heiden et al. used a zebrafish model to study the toxicity of CdSe/ZnS QDs [124]. In their study zebrafish embryos were exposed to aqueous solutions of QDs. They reported that the toxicity was influenced by the QDs coating. At sublethal doses, many QDs preparations produced characteristic signs of cadmium toxicity that weakly correlated with

metallothionein expression suggesting that QDs were slightly degraded *in vivo*. They also reported that QDs produced distinctively different toxicity that could not be described by cadmium release. In another study, Truong et al. evaluated the importance of QDs surface functionalization in both nanoparticle stability and *in vivo* biological responses using the embryonic zebrafish [125]. They used two PbS QDs formulation with the same core sizes but different surface functionalization. Exposure to these QDs was begun 6 hrs post fertilisation. They showed that QDs toxicity was strongly associated with the surface ligands.

In vivo toxicity studies of QDs have also been carried out in various mouse and rat models. For instance, Hauck et al. performed a systemic study to evaluate the effect of dosing and surface chemistry on the short- and long-term *in vivo* toxicity of CdSe/ZnS QDs in rats [126]. Animal survival, animal mass, haematological and biochemical tests, and organ histology showed that QDs did not cause appreciable toxicity under *in vivo* condition. Even chronically dosed rats did not experience QDs toxicity. In another study by Su et al., short- and long-term biodistribution and toxicity of CdTe QDs were investigated after administration into the mice [127]. They showed that QDs were initially accumulated in the liver after short-term post-injection, and then were absorbed by the kidney during long-time. Histological and biochemical analysis, and body weight measurements revealed that there was no advert effect of QDs in mice even after long-time exposure time. Gao et al. injected dendron-coated InP/ZnS QDs into the mice [80]. The dendrimer and dendron molecules have unique physicochemical properties and have great potential for use in a variety of biomedical applications including drug delivery [128]. A pilot mouse toxicity study by this group confirmed that these dendron coated QDs were not toxic at the doses tested.

Non-human primates are irreplaceable animal models for biomedical research because of their close evolutionary relationship to humans. The first study of QDs in primates was reported by Ye et al. [129]. In their study phospholipid micelle encapsulated CdSe/CdS/ZnS QDs were injected into rhesus macaques. The results revealed that the haematological and biochemical markers were within normal ranges over 90 days of monitoring. In addition histological analysis of major organs displayed no sign of inflammation or injury. However, chemical extraction of the tissues revealed that most of the initial dose of the cadmium remained in the liver, spleen and kidney after 90 days post-injection, indicating that the breakdown and clearance rate of QDs is slow in comparison to biodegradable polymer nanoparticles. This suggests that longer-term studies will be essential to determine the eventual effect of these nanoparticles in the body.

To characterise fully the *in vivo* toxicity of QDs, further comprehensive investigations are still required. Some of these assessments include the evaluation of QD composition (cadmium-based *versus* cadmium free QDs), surface chemistry, size, and shape. In future for the nonhuman primate studies of QDs toxicity, the cardiovascular and respiratory measurements would also be valuable. Specific immunohistochemistry assay can be used to hepatocytes in the liver samples. Genetic analysis such as polymerase chain reaction (q-RT-PCR) can also be performed on tissue samples to determine the inflammatory gene regulation. Future *in vivo* studies should also focus on long-term accumulation of QDs and on understanding their excretion through the feces and urine. Combining the results from all of these studies will eventually provide valuable information and guidance for the design and use of QDs in biomedical field.

Conclusions

The long-term goal in medical applications of nanobiotechnology is to design and develop nanoparticles with multiple functions that are capable of targeting diseased tissues, treating the disease and monitoring progress in real time. One of the most early applications of QDs would be in areas such as image-guided surgery for tumour removal. QDs can also be designed to develop more complex multifunctional nanostructure, such as incorporation of paramagnetic metals into the nanoparticles. In this imaging modality, QDs could be used as MRI contrast agents for the detection of deep seated tumours, while intraoperative fluorescence imaging of QDs would enable the surgeon to define the tumour margins to excise the entire tumours more completely. QDs can also be conjugated to therapeutic agents, which would enable simultaneous diagnostic imaging and drug delivery monitoring in real time. For biomedical applications, it is important to minimise the overall size of QDs, to reduce nonspecific protein adsorption, to understand the toxic effect of semiconductor materials, to develop near-infrared emitting QDs to minimise the problems of indigenous fluorescence of tissue and enhance penetration depth. For the clinical translation, QD nanoparticles should be composed of nontoxic materials and should be biodegradable. Cadmium free QDs could therefore offer the opportunity to fulfil the biological applications of QDs without the toxicity limitations encountered by cadmium containing QDs. By reaching these goals, QD nanoparticles will complement organic fluorophores deficiencies in particular applications as *in vivo* imaging.

References

1. Ferrari M: Cancer Nanotechnology: opportunities and challenges. *Nat Rev Cancer* 2005;5:161-171.
2. Alivisatos AP, Gu WW, Larabell C: Quantum dots as cellular probes. *Annual Review of Biomedical Engineering* 2005;7:55-76.
3. Brunetti V, Chibli H, Fiammengio R, Galeone A, Malvindi MA, Vecchio G, Cingolani R, Nadeau JL, Pompa PP: InP/ZnS as a safer alternative to CdSe/ZnS core/shell quantum dots: in vitro and in vivo toxicity assessment. *Nanoscale* 2013;5:307-317.
4. Dubertret B, Skourides P, Norris DJ, Noireaux V, Brivanlou AH, Libchaber A: In vivo imaging of quantum dots encapsulated in phospholipid micelles. *Science* 2002;298:1759-1762.
5. Han MY, Gao XH, Su JZ, Nie S: Quantum-dot-tagged microbeads for multiplexed optical coding of biomolecules. *Nature Biotechnology* 2001;19:631-635.
6. Parak WJ, Boudreau R, Le Gros M, Gerion D, Zanchet D, Micheel CM, Williams SC, Alivisatos AP, Larabell C: Cell motility and metastatic potential studies based on quantum dot imaging of phagokinetic tracks. *Advanced Materials* 2002;14:882-885.
7. Taylor JR, Fang MM, Nie SM: Probing specific sequences on single DNA molecules with bioconjugated fluorescent nanoparticles. *Analytical Chemistry* 2000;72:1979-1986.
8. Wu XY, Liu HJ, Liu JQ, Haley KN, Treadway JA, Larson JP, Ge NF, Peale F, Bruchez MP: Immunofluorescent labeling of cancer marker Her2 and other cellular targets with semiconductor quantum dots. *Nature Biotechnology* 2003;21:41-46.
9. Han MY, Gao XH, Su JZ, Nie S: Quantum-dot-tagged microbeads for multiplexed optical coding of biomolecules. *Nature Biotechnology* 2001;19:631-635.

10. Kairdolf BA, Smith AM, Stokes TH, Wang MD, Young AN, Nie S: Semiconductor quantum dots for bioimaging and biodiagnostic applications. *Annu Rev Anal Chem (Palo Alto Calif)* 2013;6:143-162.
11. Qu LH, Peng XG: Control of photoluminescence properties of CdSe nanocrystals in growth. *Journal of the American Chemical Society* 2002;124:2049-2055.
12. Bailey RE, Nie SM: Alloyed semiconductor quantum dots: Tuning the optical properties without changing the particle size. *Journal of the American Chemical Society* 2003;125:7100-7106.
13. Kim S, Fisher B, Eisler HY, Bawendi MG: Novel type-II quantum dots: CDTE/CDSE(core/shell) and CDSE/ZNTE(core/shell) heterostructures. *Abstracts of Papers of the American Chemical Society* 2002;224:U443.
14. Smith AM, Gao XH, Nie SM: Quantum dot nanocrystals for in vivo molecular and cellular imaging. *Photochemistry and Photobiology* 2004;80:377-385.
15. Smith AM, Gao XH, Nie SM: Quantum dot nanocrystals for in vivo molecular and cellular imaging. *Photochemistry and Photobiology* 2004;80:377-385.
16. Dabbousi BO, Rodriguez-Viejo J, Mikulec FV, Heine JR, Mattoussi H, Ober R, Jensen KF, Bawendi MG: (CdSe)ZnS Core-Shell Quantum Dots: Synthesis and Characterization of a Size Series of Highly Luminescent Nanocrystallites. *J Phys Chem B* 1997;9463-9475.
17. Hines MA, Guyot-Sionnest P: Synthesis and characterization of strongly luminescing ZnS-Capped CdSe nanocrystals. *Journal of Physical Chemistry* 1996;100:468-471.
18. Aldana A, Wang YA, Peng X: Photochemical Instability of CdSe Nanocrystals Coated by Hydrophilic Thiols. *J Am Chem Soc* 2001;8844-8850.
19. Chan WCW, Nie SM: Quantum dot bioconjugates for ultrasensitive nonisotopic detection. *Science* 1998;281:2016-2018.
20. Kim S, Bawendi MG: Oligomeric ligands for luminescent and stable nanocrystal quantum dots. *J Am Chem Soc* 2003;125:14652-14653.
21. Fan H, Leve EW, Scullin C, Gabaldon J, Tallant D, Bunge S, Boyle T, Wilson MC, Brinker CJ: Surfactant-assisted synthesis of water-soluble and biocompatible semiconductor quantum dot micelles. *Nano Lett* 2005;5:645-648.
22. Weijer CJ: Visualizing signals moving in cells. *Science* 2003;300:96-100.
23. Miyawaki A, Sawano A, Kogure T: Lighting up cells: labelling proteins with fluorophores. *Nat Cell Biol* 2003;Suppl:S1-S7.
24. Miyawaki A: Visualization of the spatial and temporal dynamics of intracellular signaling. *Developmental Cell* 2003;4:295-305.
25. Resch-Genger U, Grabolle M, Cavaliere-Jaricot S, Nitschke R, Nann T: Quantum dots versus organic dyes as fluorescent labels. *Nature Methods* 2008;5:763-775.
26. Jaiswal JK, Mattoussi H, Mauro JM, Simon SM: Long-term multiple color imaging of live cells using quantum dot bioconjugates. *Nature Biotechnology* 2003;21:47-51.
27. Voura EB, Jaiswal JK, Mattoussi H, Simon SM: Tracking metastatic tumor cell extravasation with quantum dot nanocrystals and fluorescence emission-scanning microscopy. *Nature Medicine* 2004;10:993-998.
28. Goldman ER, Clapp AR, Anderson GP, Uyeda HT, Mauro JM, Medintz IL, Mattoussi H: Multiplexed toxin analysis using four colors of quantum dot fluororeagents. *Analytical Chemistry* 2004;76:684-688.
29. Kim S, Lim YT, Soltesz EG, De Grand AM, Lee J, Nakayama A, Parker JA, Mihaljevic T, Laurence RG, Dor DM, Cohn LH, Bawendi MG, Frangioni JV: Near-infrared fluorescent type II quantum dots for sentinel lymph node mapping. *Nature Biotechnology* 2004;22:93-97.

30. Yu WW, Qu LH, Guo WZ, Peng XG: Experimental determination of the extinction coefficient of CdTe, CdSe, and CdS nanocrystals. *Chemistry of Materials* 2003;15:2854-2860.
31. Bruchez M, Moronne M, Gin P, Weiss S, Alivisatos AP: Semiconductor nanocrystals as fluorescent biological labels. *Science* 1998;281:2013-2016.
32. Hanaki K, Momo A, Oku T, Komoto A, Maenosono S, Yamaguchi Y, Yamamoto K: Semiconductor quantum dot/albumin complex is a long-life and highly photostable endosome marker. *Biochemical and Biophysical Research Communications* 2003;302:496-501.
33. Dahan M, Levi S, Luccardini C, Rostaing P, Riveau B, Triller A: Diffusion dynamics of glycine receptors revealed by single-quantum dot tracking. *Science* 2003;302:442-445.
34. Lidke DS, Nagy P, Heintzmann R, Rndt-Jovin DJ, Post JN, Grecco HE, Jares-Erijman EA, Jovin TM: Quantum dot ligands provide new insights into erbB/HER receptor-mediated signal transduction. *Nature Biotechnology* 2004;22:198-203.
35. Gao X, Cui Y, Levenson RM, Chung LW, Nie S: In vivo cancer targeting and imaging with semiconductor quantum dots. *Nat Biotechnol* 2004;22:969-976.
36. Larson DR, Zipfel WR, Williams RM, Clark SW, Bruchez MP, Wise FW, Webb WW: Water-soluble quantum dots for multiphoton fluorescence imaging in vivo. *Science* 2003;300:1434-1436.
37. Michalet X, Pinaud F, Lacoste TD, Dahan M, Bruchez MP, Alivisatos AP, Weiss S: Properties of fluorescent semiconductor nanocrystals and their application to biological labeling. *Single Molecules* 2001;2:261-276.
38. Dahan M, Laurence T, Pinaud F, Chemla DS, Alivisatos AP, Sauer M, Weiss S: Time-gated biological imaging by use of colloidal quantum dots. *Optics Letters* 2001;26:825-827.
39. Jamieson T, Bakhshi R, Petrova D, Pocock R, Imani M, Seifalian AM: Biological applications of quantum dots. *Biomaterials* 2007;28:4717-4732.
40. Ntziachristos V, Yodh AG, Schnall M, Chance B: Concurrent MRI and diffuse optical tomography of breast after indocyanine green enhancement. *Proc Natl Acad Sci U S A* 2000;97:2767-2772.
41. Ballou B, Ernst LA, Waggoner AS: Fluorescence imaging of tumors in vivo. *Curr Med Chem* 2005;12:795-805.
42. Frangioni JV: In vivo near-infrared fluorescence imaging. *Curr Opin Chem Biol* 2003;7:626-634.
43. Cassette E, Helle M, Bezdetnaya L, Marchal F, Dubertret B, Pons T: Design of new quantum dot materials for deep tissue infrared imaging. *Adv Drug Deliv Rev* 2013;65:719-731.
44. Bonnema J, van de Velde CJ: Sentinel lymph node biopsy in breast cancer. *Ann Oncol* 2002;13:1531-1537.
45. Morton DL, Wen DR, Wong JH, Economou JS, Cagle LA, Storm FK, Foshag LJ, Cochran AJ: Technical details of intraoperative lymphatic mapping for early stage melanoma. *Arch Surg* 1992;127:392-399.
46. Wood TF, Nora DT, Morton DL, Turner RR, Rangel D, Hutchinson W, Bilchik AJ: One hundred consecutive cases of sentinel lymph node mapping in early colorectal carcinoma: detection of missed micrometastases. *J Gastrointest Surg* 2002;6:322-329.
47. Barthelmes L, Goyal A, Newcombe RG, McNeill F, Mansel RE: Adverse reactions to patent blue V dye - The NEW START and ALMANAC experience. *Eur J Surg Oncol* 2010;36:399-403.
48. Tanaka E, Choi HS, Fujii H, Bawendi MG, Frangioni JV: Image-guided oncologic surgery using invisible light: completed pre-clinical development for sentinel lymph node mapping. *Ann Surg Oncol* 2006;13:1671-1681.
49. Parungo CP, Colson YL, Kim SW, Kim S, Cohn LH, Bawendi MG, Frangioni JV: Sentinel lymph node mapping of the pleural space. *Chest* 2005;127:1799-1804.

50. Soltesz EG, Kim S, Laurence RG, DeGrand AM, Parungo CP, Dor DM, Cohn LH, Bawendi MG, Frangioni JV, Mihaljevic T: Intraoperative sentinel lymph node mapping of the lung using near-infrared fluorescent quantum dots. *Ann Thorac Surg* 2005;79:269-277.
51. Parungo CP, Ohnishi S, Kim SW, Kim S, Laurence RG, Soltesz EG, Chen FY, Colson YL, Cohn LH, Bawendi MG, Frangioni JV: Intraoperative identification of esophageal sentinel lymph nodes with near-infrared fluorescence imaging. *J Thorac Cardiovasc Surg* 2005;129:844-850.
52. Soltesz EG, Kim S, Kim SW, Laurence RG, De Grand AM, Parungo CP, Cohn LH, Bawendi MG, Frangioni JV: Sentinel lymph node mapping of the gastrointestinal tract by using invisible light. *Ann Surg Oncol* 2006;13:386-396.
53. Zimmer JP, Kim SW, Ohnishi S, Tanaka E, Frangioni JV, Bawendi MG: Size series of small indium arsenide-zinc selenide core-shell nanocrystals and their application to in vivo imaging. *J Am Chem Soc* 2006;128:2526-2527.
54. Kobayashi H, Hama Y, Koyama Y, Barrett T, Regino CA, Urano Y, Choyke PL: Simultaneous multicolor imaging of five different lymphatic basins using quantum dots. *Nano Lett* 2007;7:1711-1716.
55. Ballou B, Ernst LA, Andreko S, Harper T, Fitzpatrick JA, Waggoner AS, Bruchez MP: Sentinel lymph node imaging using quantum dots in mouse tumor models. *Bioconjug Chem* 2007;18:389-396.
56. Pons T, Pic E, Lequeux N, Cassette E, Bezdetsnaya L, Guillemin F, Marchal F, Dubertret B: Cadmium-free CuInS₂/ZnS quantum dots for sentinel lymph node imaging with reduced toxicity. *ACS Nano* 2010;4:2531-2538.
57. Erogbogbo F, Yong KT, Roy I, Hu R, Law WC, Zhao W, Ding H, Wu F, Kumar R, Swihart MT, Prasad PN: In vivo targeted cancer imaging, sentinel lymph node mapping and multi-channel imaging with biocompatible silicon nanocrystals. *ACS Nano* 2011;5:413-423.
58. Jain RK: Transport of molecules, particles, and cells in solid tumors. *Annu Rev Biomed Eng* 1999;1:241-263.
59. Jain RK: Transport of molecules, particles, and cells in solid tumors. *Annu Rev Biomed Eng* 1999;1:241-263.
60. Jain RK: Delivery of molecular and cellular medicine to solid tumors. *Adv Drug Deliv Rev* 2001;46:149-168.
61. Papagiannaros A, Levchenko T, Hartner W, Mongayt D, Torchilin V: Quantum dots encapsulated in phospholipid micelles for imaging and quantification of tumors in the near-infrared region. *Nanomedicine* 2009;5:216-224.
62. Shuhendler AJ, Prasad P, Chan HK, Gordijo CR, Soroushian B, Kolios M, Yu K, O'Brien PJ, Rauth AM, Wu XY: Hybrid quantum dot-fatty ester stealth nanoparticles: toward clinically relevant in vivo optical imaging of deep tissue. *ACS Nano* 2011;5:1958-1966.
63. Popovic Z, Liu W, Chauhan VP, Lee J, Wong C, Greytak AB, Insin N, Nocera DG, Fukumura D, Jain RK, Bawendi MG: A nanoparticle size series for in vivo fluorescence imaging. *Angew Chem Int Ed Engl* 2010;49:8649-8652.
64. Choi HS, Liu W, Misra P, Tanaka E, Zimmer JP, Itty IB, Bawendi MG, Frangioni JV: Renal clearance of quantum dots. *Nat Biotechnol* 2007;25:1165-1170.
65. Choi HS, Liu W, Liu F, Nasr K, Misra P, Bawendi MG, Frangioni JV: Design considerations for tumour-targeted nanoparticles. *Nat Nanotechnol* 2010;5:42-47.
66. Yu.x, Chen.L, Li.K, Li.Y, Xiao.S, Liu.J, Zhou.L: Immunofluorescence detection with quantum dot bioconjugates for hepatoma in vivo. *Journal of Biomedical Optics* 2007.

67. Tada H, Higuchi H, Wanatabe TM, Ohuchi N: In vivo real-time tracking of single quantum dots conjugated with monoclonal anti-HER2 antibody in tumors of mice. *Cancer Res* 2007;67:1138-1144.
68. Baselga J: Targeting tyrosine kinases in cancer: the second wave. *Science* 2006;312:1175-1178.
69. Blume-Jensen P, Hunter T: Oncogenic kinase signalling. *Nature* 2001;411:355-365.
70. Yang L, Mao H, Wang YA, Cao Z, Peng X, Wang X, Duan H, Ni C, Yuan Q, Adams G, Smith MQ, Wood WC, Gao X, Nie S: Single chain epidermal growth factor receptor antibody conjugated nanoparticles for in vivo tumor targeting and imaging. *Small* 2009;5:235-243.
71. Akerman ME, Chan WCW, Laakkonen P, Bhatia SN, Ruoslahti E: Nanocrystal targeting in vivo. *Proceedings of the National Academy of Sciences of the United States of America* 2002;99:12617-12621.
72. Pedchenko V, Zent R, Hudson BG: Alpha(v)beta3 and alpha(v)beta5 integrins bind both the proximal RGD site and non-RGD motifs within noncollagenous (NC1) domain of the alpha3 chain of type IV collagen: implication for the mechanism of endothelia cell adhesion. *J Biol Chem* 2004;279:2772-2780.
73. Zitzmann S, Ehemann V, Schwab M: Arginine-glycine-aspartic acid (RGD)-peptide binds to both tumor and tumor-endothelial cells in vivo. *Cancer Res* 2002;62:5139-5143.
74. Hood JD, Cheresch DA: Role of integrins in cell invasion and migration. *Nat Rev Cancer* 2002;2:91-100.
75. Cai W, Shin DW, Chen K, Gheysens O, Cao Q, Wang SX, Gambhir SS, Chen X: Peptide-labeled near-infrared quantum dots for imaging tumor vasculature in living subjects. *Nano Lett* 2006;6:669-676.
76. Gao J, Chen.K, Xie.R, Xie.J, Yan.Y, Cheng.Z, Peng.X, Chen.X: In vivo tumour-targeted fluorescence imaging using near-infrared non-cadmium quantum dots. *Bioconjugate Chemistry* 2010;604-609.
77. Cai W, Chen K, Li ZB, Gambhir SS, Chen X: Dual-function probe for PET and near-infrared fluorescence imaging of tumor vasculature. *J Nucl Med* 2007;48:1862-1870.
78. Park JH, Gu L, von MG, Ruoslahti E, Bhatia SN, Sailor MJ: Biodegradable luminescent porous silicon nanoparticles for in vivo applications. *Nat Mater* 2009;8:331-336.
79. Gao J, Chen K, Xie R, Xie J, Lee S, Cheng Z, Peng X, Chen X: Ultrasmall near-infrared non-cadmium quantum dots for in vivo tumor imaging. *Small* 2010;6:256-261.
80. Gao J, Chen K, Luong R, Bouley DM, Mao H, Qiao T, Gambhir SS, Cheng Z: A Novel Clinically Translatable Fluorescent Nanoparticle for Targeted Molecular Imaging of Tumors in Living Subjects. *Nano Lett* 2011.
81. Smith BR, Cheng Z, De A, Koh AL, Sinclair R, Gambhir SS: Real-time intravital imaging of RGD-quantum dot binding to luminal endothelium in mouse tumor neovasculature. *Nano Letters* 2008;8:2599-2606.
82. So MK, Xu C, Loening AM, Gambhir SS, Rao J: Self-illuminating quantum dot conjugates for in vivo imaging. *Nat Biotechnol* 2006;24:339-343.
83. Xing Y, So MK, Koh AL, Sinclair R, Rao J: Improved QD-BRET conjugates for detection and imaging. *Biochem Biophys Res Commun* 2008;372:388-394.
84. Xia Z, Rao J: Biosensing and imaging based on bioluminescence resonance energy transfer. *Curr Opin Biotechnol* 2009;20:37-44.
85. Wilson T, Hastings JW: Bioluminescence. *Annu Rev Cell Dev Biol* 1998;14:197-230.
86. De A, Gambhir SS: Noninvasive imaging of protein-protein interactions from live cells and living subjects using bioluminescence resonance energy transfer. *FASEB J* 2005;19:2017-2019.

87. Louie A: Multimodality imaging probes: design and challenges. *Chem Rev* 2010;110:3146-3195.
88. Wang S, Jarrett BR, Kauzlarich SM, Louie AY: Core/shell quantum dots with high relaxivity and photoluminescence for multimodality imaging. *J Am Chem Soc* 2007;129:3848-3856.
89. Li L, Choo ESG, Liu Z, Ding J, Xue J: Double-layer silica core-shell nanospheres with superparamagnetic and fluorescent functionalities. *Chem Phys Lett* 2008;461:114-117.
90. Zhang B, Cheng J, Gong X, Dong X, Liu X, Ma G, Chang J: Facile fabrication of multi-colors high fluorescent/superparamagnetic nanoparticles. *J Colloid Interface Sci* 2008;322.
91. Wilson R, Spiller DG, Prior IA, Bhatt A, Hutchinson A: Magnetic microspheres encoded with photoluminescent quantum dots for multiplexed detection. *J Mater Chem* 2007;17:4400-4406.
92. Cai W, Chen X: Nanoplatforms for Targeted Molecular Imaging in Living Subjects. *Small* 2007;1840-1854.
93. Bagalkot V, Zhang L, Levy-Nissenbaum E, Jon S, Kantoff PW, Langer R, Farokhzad OC: Quantum dot-aptamer conjugates for synchronous cancer imaging, therapy, and sensing of drug delivery based on bi-fluorescence resonance energy transfer. *Nano Lett* 2007;7:3065-3070.
94. Dolmans DEJG, Fukumura D, Jain RK: Photodynamic therapy for cancer. *Nature Reviews Cancer* 2003;3:380-387.
95. MacDonald IJ, Dougherty TJ: Basic principles of photodynamic therapy. *Journal of Porphyrins and Phthalocyanines* 2001;5:105-129.
96. Pandey RK: Recent advances in photodynamic therapy. *Journal of Porphyrins and Phthalocyanines* 2000;4:368-373.
97. Battah S, Balaratnam S, Casas A, O'Neill S, Edwards C, Batlle A, Dobbin P, MacRobert AJ: Macromolecular delivery of 5-aminolaevulinic acid for photodynamic therapy using dendrimer conjugates. *Molecular Cancer Therapeutics* 2007;6:876-885.
98. Chen W: Nanoparticle Self-Lighting Photodynamic Therapy for Cancer Treatment. *Biomedical Nanotechnology* 2008.
99. Imahori H, Arimura M, Hanada T, Nishimura Y, Yamazaki I, Sakata Y, Fukuzumi S: Photoactive three-dimensional monolayers: Porphyrin-alkanethiolate-stabilized gold clusters. *Journal of the American Chemical Society* 2001;123:335-336.
100. Roy I, Ohulchanskyy TY, Pudavar HE, Bergey EJ, Oseroff AR, Morgan J, Dougherty TJ, Prasad PN: Ceramic-based nanoparticles entrapping water-insoluble photosensitizing anticancer drugs: A novel drug-carrier system for photodynamic therapy. *Journal of the American Chemical Society* 2003;125:7860-7865.
101. Wang SZ, Gao RM, Zhou FM, Selke M: Nanomaterials and singlet oxygen photosensitizers: potential applications in photodynamic therapy. *Journal of Materials Chemistry* 2004;14:487-493.
102. Wieder ME, Hone DC, Cook MJ, Handsley MM, Gavrilovic J, Russell DA: Intracellular photodynamic therapy with photosensitizer-nanoparticle conjugates: cancer therapy using a 'Trojan horse'. *Photochemical & Photobiological Sciences* 2006;5:727-734.
103. Konan YN, Gurny R, Allemann E: State of the art in the delivery of photosensitizers for photodynamic therapy. *Journal of Photochemistry and Photobiology B-Biology* 2002;66:89-106.
104. Yaghini E, Seifalian AM, MacRobert AJ: Quantum dots and their potential biomedical applications in photosensitization for photodynamic therapy. *Nanomedicine* 2009;4:353-363.

105. Samia ACS, Chen XB, Burda C: Semiconductor quantum dots for photodynamic therapy. *Journal of the American Chemical Society* 2003;125:15736-15737.
106. Samia ACS, Dayal S, Burda C: Quantum dot-based energy transfer: Perspectives and potential for applications in photodynamic therapy. *Photochemistry and Photobiology* 2006;82:617-625.
107. Shi LX, Hernandez B, Selke M: Singlet oxygen generation from water-soluble quantum dot-organic dye nanocomposites. *Journal of the American Chemical Society* 2006;128:6278-6279.
108. Tsay JM, Trzoss M, Shi LX, Kong XX, Selke M, Jung ME, Weiss S: Singlet oxygen production by peptide-coated quantum dot-photosensitizer conjugates. *Journal of the American Chemical Society* 2007;129:6865-6871.
109. Lei Y, Tang H, Yao L, Yu R, Feng M, Zou B: Applications of mesenchymal stem cells labeled with Tat peptide conjugated quantum dots to cell tracking in mouse body. *Bioconjugate Chemistry* 2008;19:421-427.
110. Rosen AB, Kelly DJ, Schuldt AJ, Lu J, Potapova IA, Doronin SV, Robichaud KJ, Robinson RB, Rosen MR, Brink PR, Gaudette GR, Cohen IS: Finding fluorescent needles in the cardiac haystack: tracking human mesenchymal stem cells labeled with quantum dots for quantitative in vivo three-dimensional fluorescence analysis. *Stem Cells* 2007;25:2128-2138.
111. Voura EB, Jaiswal JK, Mattoussi H, Simon SM: Tracking metastatic tumor cell extravasation with quantum dot nanocrystals and fluorescence emission-scanning microscopy. *Nature Medicine* 2004;10:993-998.
112. Moghimi SM, Szebeni J: Stealth liposomes and long circulating nanoparticles: critical issues in pharmacokinetics, opsonization and protein-binding properties. *Prog Lipid Res* 2003;42:463-478.
113. Choi HS, Ipe BI, Misra P, Lee JH, Bawendi MG, Frangioni JV: Tissue- and organ-selective biodistribution of NIR fluorescent quantum dots. *Nano Lett* 2009;9:2354-2359.
114. Fischer HCLPKSCW, .: Pharmacokinetics of Nanoscale Quantum Dots: In Vivo Distribution, Sequestration, and Clearance in the Rat. *Advanced Functional Materials* 2006.
115. Ballou B, Lagerholm BC, Ernst LA, Bruchez MP, Waggoner AS: Noninvasive imaging of quantum dots in mice. *Bioconjugate Chemistry* 2004;15:79-86.
116. Al-Jamal WT, Al-Jamal KT, Cakebread A, Halket JM, Kostarelos K: Blood circulation and tissue biodistribution of lipid-quantum dot (L-QD) hybrid vesicles intravenously administered in mice. *Bioconjug Chem* 2009;20:1696-1702.
117. Cho SJ, Maysinger D, Jain M, Roder B, Hackbarth S, Winnik FM: Long-term exposure to CdTe quantum dots causes functional impairments in live cells. *Langmuir* 2007;23:1974-1980.
118. Derfus AM, Chan WCW, Bhatia SN: Probing the cytotoxicity of semiconductor quantum dots. *Nano Letters* 2004;4:11-18.
119. Hardman R: A toxicologic review of quantum dots: toxicity depends on physicochemical and environmental factors. *Environ Health Perspect* 2006;114:165-172.
120. Hoshino A, Fujioka K, Oku T, Suga M, Sasaki YF, Ohta T, Yasuhara M, Suzuki K, Yamamoto K: Physicochemical properties and cellular toxicity of nanocrystal quantum dots depend on their surface modification. *Nano Letters* 2004;4:2163-2169.
121. Kirchner C, Liedl T, Kudera S, Pellegrino T, Javier AM, Gaub HE, Stolze S, Fertig N, Parak WJ: Cytotoxicity of colloidal CdSe and CdSe/ZnS nanoparticles. *Nano Letters* 2005;5:331-338.
122. Cooper DR, Dimitrijevic NM, Nadeau JL: Photosensitization of CdSe/ZnS QDs and reliability of assays for reactive oxygen species production. *Nanoscale* 2010;2:114-121.
123. Yong KT, Law WC, Hu R, Ye L, Liu L, Swihart MT, Prasad PN: Nanotoxicity assessment of quantum dots: from cellular to primate studies. *Chem Soc Rev* 2013;42:1236-1250.

124. King-Heiden TC, Wiecinski PN, Mangham AN, Metz KM, Nesbit D, Pedersen JA, Hamers RJ, Heideman W, Peterson RE: Quantum dot nanotoxicity assessment using the zebrafish embryo. *Environ Sci Technol* 2009;43:1605-1611.
125. Truong L, Moody IS, Stankus DP, Nason JA, Lonergan MC, Tanguay RL: Differential stability of lead sulfide nanoparticles influences biological responses in embryonic zebrafish. *Arch Toxicol* 2011;85:787-798.
126. Hauck TS, Anderson RE, Fischer HC, Newbigging S, Chan WC: In vivo quantum-dot toxicity assessment. *Small* 2010;6:138-144.
127. Su Y, Peng F, Jiang Z, Zhong Y, Lu Y, Jiang X, Huang Q, Fan C, Lee ST, He Y: In vivo distribution, pharmacokinetics, and toxicity of aqueous synthesized cadmium-containing quantum dots. *Biomaterials* 2011;32:5855-5862.
128. Astruc D, Boisselier E, Ornelas C: Dendrimers designed for functions: from physical, photophysical, and supramolecular properties to applications in sensing, catalysis, molecular electronics, photonics, and nanomedicine. *Chem Rev* 2010;110:1857-1959.
129. Ye L, Yong KT, Liu L, Roy I, Hu R, Zhu J, Cai H, Law WC, Liu J, Wang K, Liu J, Liu Y, Hu Y, Zhang X, Swihart MT, Prasad PN: A pilot study in non-human primates shows no adverse response to intravenous injection of quantum dots. *Nat Nanotechnol* 2012;7:453-458.